UC Irvine
UC Irvine Previously Published Works

Title

Engineered D2R Variants Reveal the Balanced and Biased Contributions of G-Protein and β-Arrestin to Dopamine-Dependent Functions

Permalink

https://escholarship.org/uc/item/8dq57618

Journal

Neuropsychopharmacology, 43(5)

ISSN

0893-133X

Authors

Rose, Samuel J
Pack, Thomas F
Peterson, Sean M
et al.

Publication Date

2018-04-01

DOI

10.1038/npp.2017.254

Peer reviewed

Engineered D2R Variants Reveal the Balanced and Biased Contributions of G-Protein and β-Arrestin to Dopamine-Dependent Functions

Samuel J Rose[1], Thomas F Pack[1], Sean M Peterson[1], Kaitlin Payne[1], Emiliana Borrelli[2] and Marc G Caron[*,1,3]

[1]Department of Cell Biology, Duke University Medical Center, Durham, NC, USA; [2]Department of Microbiology and Molecular Genetics, University of California, Irvine, Irvine, CA, USA; [3]Department of Medicine and Neurobiology, Duke University Medical Center, Durham, NC, USA

The dopamine D2 receptor (D2R), like many G-protein-coupled receptors, signals through G-protein- and β-arrestin-dependent pathways. Preferential activation of one of these pathways is termed functional selectivity or biased signaling and is a promising therapeutic strategy. Though biased signaling through D2Rs has been demonstrated, acquiring the mechanistic details of biased D2R/G-protein and D2R/β-arrestin signaling *in vivo* has been challenging because of the lack of techniques that specifically target these interactions in discrete cell populations. To address this question, we employed a cell type-specific viral expression approach to restore D2R variants that preferentially engage either G-protein or β-arrestin signaling in 'indirect pathway' medium spiny neurons (iMSNs), because of their central role in dopamine circuitry. We found that the effect of haloperidol antagonism on D2R metabolic signaling events is largely mediated by acute blockade of D2R/G-protein signaling. We show that a D2R-driven behavior, nestlet shredding, is similarly driven by D2R/G-protein signaling. On the other hand, D2R-driven locomotion and rearing require coordinated D2R/G-protein and D2R/β-arrestin signaling. The acute locomotor response to amphetamine and cocaine similarly depend on both G-protein and β-arrestin D2R signaling. Surprisingly, another psychotropic drug, phencyclidine, displayed a selective D2R/β-arrestin potentiation of locomotion. These findings highlight how D2R mostly relies upon balanced G-protein and β-arrestin signaling in iMSNs. However, the response to haloperidol and phencyclidine indicates that normal D2R signaling homeostasis can be dramatically altered, indicating that targeting a specific D2R signal transduction pathway could allow for more precise modulation of dopamine circuit function.

INTRODUCTION

Dysfunction of dopamine D2 receptor (D2R) signaling is implicated in many neurological and psychiatric disorders including schizophrenia, attention deficit hyperactivity disorder, and Parkinson's disease. Compounds that modulate dopamine levels or target D2R directly have been intensely pursued for several decades (Seeman *et al*, 1976; Carlsson, 1978; Weinberger, 1987; Kane *et al*, 1988) with many successfully clinical treatments in wide use. It is now well recognized that G-protein-coupled receptors (GPCRs), which includes the D2R, signal through G-protein-dependent and G-protein-independent mechanisms. Gαi/o-mediated D2R signaling inhibits adenylyl cyclase and cyclic adenosine monophosphate (cAMP) production (Kebabian and Calne, 1979; Nishi *et al*, 1997). G-protein-independent D2R signaling, however, is initiated by GPCR-kinase (GRK)-dependent phosphorylation of D2R, and the subsequent interaction of D2R with the multifunctional adaptor protein β-arrestin2. Along with desensitizing G-protein-dependent signaling, the D2R/β-arrestin2 interaction initiates signaling in its own right (Beaulieu *et al*, 2005; Urs *et al*, 2012). In certain instances, a single ligand for a GPCR, including some examples for D2R, can serve as an agonist to one of these pathways, but not the other. This selective activation of a given pathway is termed functional selectivity or biased signaling and represents a promising pharmacotherapeutic strategy (Bohn *et al*, 2000; Allen *et al*, 2011; Whalen *et al*, 2011). Indeed, functionally selective D2R ligands would fulfill an unmet need because of the relatively poor efficacy and broad side-effect profile of existing D2R ligands (Lieberman *et al*, 2005).

Harnessing the therapeutic potential of functionally selective D2R signaling requires a better understanding of D2R signaling bias in relevant neural cell types, where the biased signaling profile of a receptor is determined by the expression level of GRKs, arrestins, and likely many other factors (Urs *et al*, 2016). Complicating this effort, D2Rs are expressed in many brain regions, including cortex, hypothalamus, amygdala, midbrain, and striatum (Weiner *et al*,

*Correspondence: Professor MG Caron, Department of Cell Biology, Duke University Medical Center, 487 CARL Building, Research Drive, Durham NC 27710, USA, Tel: +1 919 684 5433, Fax: +1 919 681 8641, E-mail: marc.caron@duke.edu

1991). In the striatum alone, D2Rs are expressed by several cell types including cholinergic interneurons (Kharkwal *et al*, 2016a), γ-aminobutyric acid (GABA)-ergic interneurons (Centonze *et al*, 2003), projections from midbrain dopaminergic neurons (Bello *et al*, 2011), as well as on medium spiny neurons (also known as spiny projection neurons) that project to the so-called 'indirect pathway' (iMSNs) in the classical go-no-go basal ganglia model (Alexander *et al*, 1986; Gerfen *et al*, 1990). Though D2Rs play an important role for each of these cell types, recent studies using cell type-specific knockouts illustrate the necessity of D2Rs expressed by iMSNs (iMSN-D2Rs) for many behavioral and physiological functions (Dobbs *et al*, 2016; Kharkwal *et al*, 2016b; Lemos *et al*, 2016). iMSN-D2R knockout mice mimic whole-body D2R knockout mice in that they exhibit deficits in locomotion, skilled movements, and the acute response to cocaine (Baik *et al*, 1995). Therefore, we sought to define the contributions of D2R/G-protein and D2R/β-arrestin signaling in iMSNs with respect to behavior, antipsychotic, and psychotropic responses in mice.

To investigate functionally selective signaling in iMSN-D2Rs, we combined cell type-specific knockout with our recently characterized biased D2R variants (Peterson *et al*, 2015) for a viral reconstitution approach. We first used a Cre-lox approach to delete D2Rs in iMSNs. Then we re-expressed D2R variants engineered to preferentially engage either D2R/G-protein (mostly Gαi/o) or D2R/β-arrestin (mostly β-arrestin2) signaling. This viral reconstitution approach allows for cell type-specific manipulation, an advantage over most pharmacological approaches. Furthermore, this approach targets only the interaction between G-protein and β-arrestin with D2Rs, an advantage over gene knockout approaches that disrupt the signaling of other GPCRs. Furthermore, with side-by-side investigation of both biased D2R variants, this approach allows for an impartial comparison between D2R/G-protein and D2R/β-arrestin signaling with regard to their functional effects. Through this approach, we evaluate how D2R undergoes alterations to the balance between G-protein and β-arrestin signaling under various physiological states.

MATERIALS AND METHODS

Mouse Lines

All animal studies were conducted in accordance with the Duke University Institutional Animal Care and Use Committee and in accordance with the NIH guidelines. $Drd2^{flox/flox}::Adora2A-Cre^{+/-}$ (iMSN-D2^{KO}) and $Drd2^{flox/flox}$ littermates (Cre-controls), on a C57BL/6J background, were generated as previously described (Urs *et al*, 2016). Male and female adult mice (2–6 months of age) were used for all studies. Animals were housed in a 12 h light/dark cycle in temperature- and humidity-controlled environment with food and water access *ad libitum*.

Viral Vectors and Stereotaxic Surgeries

D2R expression vectors were similar to those in Peterson *et al* (2015), with slight modifications. Briefly, a gene block (Integrated DNA Technologies, Coralville, IA) was designed containing mCerulean-P2A-HA sequences flanked by 5′

*Kpn*I and 3′ *Bam*HI sites and was cloned into the pcDNA3.1 vector. Then, the WT and mutant D2Rs were PCR amplified with primers adding 5′ *Bam*HI and 3′ *Eco*RI sites and then ligated into the above vector. This construct was then cut and ligated in the reverse orientation using the *Nhe*I and *Asc*I sites in a pAAV-DIO vector.

Constructs were packaged into adeno-associated virus (AAV) pseudotype 10 using the triple-transfection technique, as previously described (Xiao *et al*, 1998). Titers of each virus were determined to be between 1×10^{12} and 1×10^{13} vector genomes/ml using qPCR.

With mice anesthetized under 2% isoflurane, viruses were delivered at AP = +1.1 mm, ML = ± 1.7 mm, DV = − 2.9 mm (dorsal striatum), and − 4.0 mm (ventral striatum). To each site, 0.75 μl was delivered bilaterally. Mice were allowed to recover for 2 weeks before any experimentation.

Drugs

D-Amphetamine, cocaine HCl, and phencyclidine HCl were obtained from Sigma-Aldrich (St Louis, MO), dissolved in sterile 0.9% saline, and delivered i.p. at 10 ml/kg bodyweight. Haloperidol (Sigma-Aldrich) was dissolved in minimal glacial acetic acid and brought to volume in saline. pH was adjusted to 6.0 with NaOH and was delivered i.p. at 5 ml/kg.

Histology

Histological procedures are detailed in the Supplementary Materials and Methods. To estimate the volume of striatum with viral expression, every sixth brain section was imaged at × 12 with an AxioZoom v16 microscope equipped with Zen image acquisition software (Zeiss, Oberkochen, Germany). Using NIH ImageJ software (Bethesda, MD), a blinded observer traced the striatum according to a mouse brain atlas, along with the portion of striatum that had mCerulean+ expression. Percentage volume with expression was estimated by dividing the mCerulean+ area, in mm^2, by total striatal area, in mm^2. The intensity of HA+ immunostaining was measured using the ImageJ mean gray value measure, where gray value was assessed following black and white conversion of the image and background subtraction.

For signaling experiments, 1 : 500 dilutions of Rabbit anti-c-fos (Santa Cruz Biotechnology, Santa Cruz, CA), Rabbit anti-phospho-H3 (Ser10) (Cell Signaling Technology), Rabbit anti-Jun (Cell Signaling Technology), Rabbit anti-egr1 (Santa Cruz Biotechnology), and Rabbit anti-phospho S6 (Ser235/236) (Cell Signaling Technology) were used to label cellular markers. The × 125 double-labeled images were taken on an AxioZoom v16 microscope. Cell counting was carried by an observer blind to treatment and viral group and at least 65 mCerulean+ neurons were counted per animal. ImageJ software was used to determine whether mCerulean+ neurons contained marker labeling with fluorescence intensity values × 2 greater than background that was defined by the average fluorescence intensity value of 10 reference cells without marker labeling. Fluorescence intensity values in each mCerulean+ neuron, not corrected for background, was also analyzed.
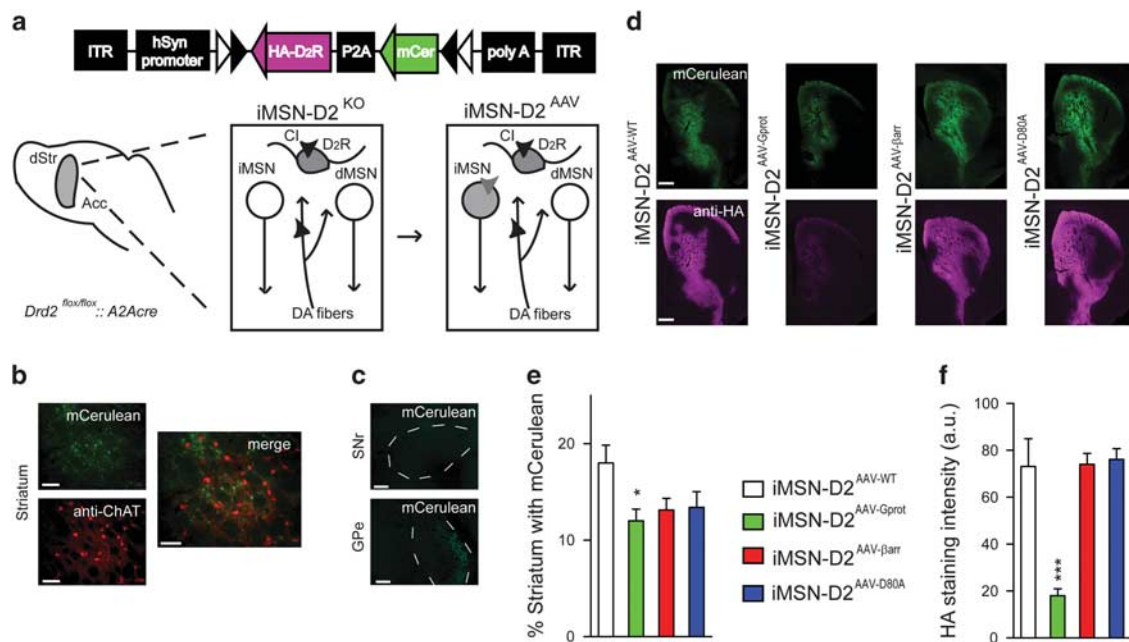
Figure 1 Viral restoration approach for expressing biased D2R variants in iMSNs. (a) Schematic of a viral transgene packaged in AAV, containing a double-floxed inverted open reading frame. $Drd2^{flox/flox}::A2Acre$ (iMSN-D2^{KO}) mice lack endogenous D2R expression in iMSNs while simultaneously allowing Cre-dependent expression of viral transgenes in iMSNs. AAVs induce expression of HA-tagged D2R variants (purple) and label iMSNs with mCerulean. (b) No colocalization between mCerulean+ and ChAT+ neurons (scale bar = 100 μm). (c) mCerulean labels iMSN (striatopallidal) projections in external globus pallidus (GPe), but not dMSN (striatonigral) projections in substantia nigra pars reticulate (SNr) (scale bar = 500 μm). (d) Representative images of mCerulean (top) and HA immunostaining (bottom) in the rostral striatum of iMSN-D2^{AAV-WT}, iMSN-D2$^{AAV-\beta arr}$, iMSN-D2$^{AAV-Gprot}$, and iMSN-D2$^{AAV-D80A}$ mice (scale bar = 500 μm). (e) The extent that each virus was expressed was quantified by measuring the volume of dorsal and ventral striatum with expression of mCerulean. iMSN-D2^{AAV-WT} ($n=6$), iMSN-D2$^{AAV-\beta arr}$ ($n=7$), and iMSN-D2$^{AAV-D80A}$ mice ($n=5$) showed similar percent striatum with mCerulean, whereas iMSN-D2$^{AAV-Gprot}$ ($n=7$) showed slightly less striatal volume with expression (ANOVA with Bonferroni *post hoc* test, *$p<0.05$). (f) HA immunostaining intensity was quantified as a measure of D2R expression. Whereas iMSN-D2^{AAV-WT} ($n=6$), iMSN-D2$^{AAV-\beta arr}$ ($n=7$), and iMSN-D2$^{AAV-D80A}$ mice ($n=5$) do not differ, HA immunostaining intensity was significantly reduced in iMSN-D2$^{AAV-Gprot}$ ($n=7$) (ANOVA with Bonferroni *post hoc* test, ***$p<0.001$). Values represent mean ± SEM.

Locomotor Activity

Open-field activity was measured in an Accuscan activity monitor (Omnitech Electronics, Columbus, OH) and performed as previously described (Urs *et al*, 2012). Briefly, unstimulated open field locomotor activity was measured in 20 min increments over 60 min in drug-naive mice. For drug challenges, after 30 min of acclimation, drugs were injected, and mice returned to the open field. Locomotor activity was measured in 5 min intervals over 120 min.

Nestlet Shredding

Nestlet shredding was performed as previously described (Li *et al*, 2006). Briefly, mice were placed in a clean cage with a preweighed 4 cm × 4 cm cotton nestlet (~2 g). After 3 h, the amount of shredded nestlet was determined by weighing the remaining nestlet.

Statistical Analyses

Data were analyzed by standard one and two-way ANOVA and repeated-measures ANOVA tests; individual genotypes and viral groups were compared using *post hoc* Bonferroni's test in Graphpad Prism software (La Jolla, CA). Principal components analysis (PCA) was performed using JMP software (SAS, Cary, NC).

RESULTS

Viral Restoration Strategy

In order to impartially evaluate the functional consequences of biased D2R signaling in iMSNs, we used a viral restoration approach with biased D2R variants. First, mice carrying the conditional *Drd2* allele ($Drd2^{flox/flox}$) were crossed with BAC transgenic *Adora2A-Cre$^{+/-}$*mice to create mice lacking D2Rs in iMSN (iMSN-D2^{KO} mice), while preserving D2R expression in all other cell types. Next, bilateral stereotactical injections of the AAV vectors into the dorsal (caudate–putamen) and ventral striatum (nucleus accumbens) drove expression of a vector containing a human synapsin-1 promotor-driven double-floxed inverted ORF (DIO), the GFP variant mCerulean, a self-cleaving P2A sequence, and one of four HA-tagged mouse D2R variants in iMSNs (Figure 1a). The four D2R variants were identical to those published by Peterson *et al* (2015), wild-type ($^{[WT]}$D2R), a β-arrestin signaling-biased variant ($^{[A135R,M140D]}$D2R; $^{[\beta arr]}$D2R), a G-protein signaling-biased variant ($^{[L125N,}$ $^{Y133L]}$D2R; $^{[Gprot]}$D2R), and a signaling-deficient point mutant ($^{[D80A]}$D2R) for a negative control. The four groups of mice (iMSN-D2^{AAV-WT}, iMSN-D2$^{AAV-Gprot}$, iMSN-D2$^{AAV-\beta arr}$, and iMSN-D2$^{AAV-D80A}$) differed only in the D2R variant their iMSNs express, and did not express endogenous iMSN-D2Rs.

To verify exclusivity of expression in iMSNs, we examined mCerulean+ cells in striatal tissue sections that were immunostained with choline acetyl transferase (ChAT), a marker for cholinergic interneurons (Kharkwal et al, 2016a). We observed no colocalization between ChAT+ and mCerelean+ cells (Figure 1b; $n = 25$ ChAT+, $n = 138$ mCerulean+ neurons counted). iMSNs project to external globus pallidus (GPe), whereas direct pathway MSNs that express D1Rs (dMSNs) project to substantia nigra reticulate (SNr) (Alexander et al, 1986). Exploiting this projection pattern, we looked for mCerulean+ axonal fibers in these two nuclei. As expected, mCerulean+ axonal fibers were observed in GPe, but not SNr, illustrating the specificity of transgene expression to the iMSN subtype (Figure 1c). Taken together, these data confirm viral expression was specific to iMSNs.

Next, we sought to quantify D2R expression in each of the iMSN-D2R[AAV] groups. When expressed in HEK293T cells or overexpressed in iMSNs, the functionally selective variants show differences in membrane expression, and thus differences in D2R expression were expected in the iMSN-D2R[AAV] groups. However, changes in expression levels do not appear to significantly affect the pharmacological fidelity (trafficking, ligand binding, signal transduction) of the receptor variants in HEK293T cells (Peterson et al, 2015). We measured receptor expression in each of the iMSN-D2R[AAV] groups by immunostaining for the N-terminal HA tag on each receptor variant (Figure 1d). iMSN-D2[AAV-WT], iMSN-D2[AAV-βarr], and iMSN-D2[AAV-D80A] mice had similar expression of mCerulean and HA immunostaining intensity (Figure 1e and f), with robust expression in rostral dorsomedial and ventromedial striatum (including nucleus accumbens) targeted by the stereotaxic coordinates (Figure 1d). Interestingly, iMSN-D2[AAV-Gprot] mice showed significantly less expression of mCerulean ($F_{3, 21} = 3.30$, $p < 0.05$; Figure 1e) and HA immunostaining intensity ($F_{3, 21} = 19.6$, $p < 0.001$; Figure 1f). Comparatively lower expression of the [Gprot]D2R mutant was also seen in the overexpression model (Peterson et al, 2015), and likely reflects compensatory downregulation of D2R in the absence of β-arrestin-mediated desensitization of signaling. These differences in D2R expression present a significant caveat for the interpretation of our data, though we did not observe an association between behavior and expression level (Supplementary Figure S1), arguing that D2R expression level, once above a certain threshold, is not the primary factor for dopamine-driven functions. Furthermore, we wanted to avoid manipulating [Gprot]D2R levels because compensatory downregulation may be a way for the cell to avoid toxic levels of signaling. Thus, the iMSN-D2R[AAV] groups display different, but expected, levels of expression.

D2R Antagonist-Induced Signaling Is Mostly Mediated by D2R/G-Protein Blockade

To impartially investigate D2R signaling in the iMSN-D2R[AAV] groups, we examined the expression of five cellular response markers following systemic haloperidol administration: c-fos, phospho-Ser-235/236 ribosomal protein S6 (pS6), phospho-Ser-10 histone H3 (pH3), early growth response-1 (egr-1), and Jun proto-oncogene (c-Jun). These markers are well-established responses to the D2R antagonist haloperidol (Rogue and Vincendon, 1992; Bertran-Gonzalez

et al, 2008; Valjent et al, 2011; Kharkwal et al, 2016a), though each of these markers is downstream of different combinations of signaling pathways (Sheng and Greenberg, 1990; Bertran-Gonzalez et al, 2009; Bonito-Oliva et al, 2013; Bahrami and Drablos, 2016). Thus, we hypothesized that as D2R/G-protein and D2R/β-arrestin signaling activate distinct signaling pathways, distinct combinations of cellular response markers in iMSN-D2R[AAV] groups might be present following haloperidol. We treated the four iMSN-D2[AAV] groups with vehicle, 0.5 mg/kg, or 2 mg/kg haloperidol, harvested the brain 1 h later, and quantified responses in transfected iMSNs by counting colabeled mCerulean+ and cell response marker+ cells (Figure 2a–e). As a secondary quantification method we measured fluorescence intensity of the cell response markers in each cell counted (Supplementary Figure S2). As haloperidol could activate markers through off-target receptors, the inactive iMSN-D2[AAV-D80A] group provided an important control. Thus, expression of a given marker was deemed statistically significant only when an active D2R variant was different from within-group saline treatment and haloperidol-treated iMSN-D2[AAV-D80A] mice. Haloperidol at 0.5 mg/kg caused a significant increase of c-fos in iMSN-D2[AAV-WT] mice (interaction, $F_{6, 42} = 2.73$, $p < 0.01$; Figure 2a) and pS6 in iMSN-D2[AAV-WT] mice (interaction, $F_{6, 42} = 2.99$, $p < 0.01$; Figure 2b), but not in iMSN-D2[AAV-Gprot] or iMSN-D2[AAV-βarr] mice. Haloperidol at 0.5 mg/kg did not significantly alter pH3, egr-1, or c-Jun expression in any of the groups. Haloperidol at 2 mg/kg caused c-fos ($p < 0.001$), pS6 ($p < 0.001$), egr-1 (viral genotype, $F_{3, 42} = 3.59$, $p < 0.01$; Figure 2d), and c-Jun (interaction, $F_{6, 42} = 6.48$, $p < 0.001$; Figure 2e) but not pH3 expression in iMSN-D2[AAV-WT] mice. In iMSN-D2[AAV-Gprot] mice, 2 mg/kg haloperidol significantly increased pH3 (interaction, $F_{6, 42} = 10.5$, $p < 0.01$), pS6 ($p < 0.01$), egr-1 ($p < 0.05$), and c-Jun ($p < 0.001$) but not c-fos. In iMSN-D2[AAV-βarr] mice, only egr-1 ($p < 0.05$; Figure 2d) was increased by 2 mg/kg haloperidol. We further analyzed responses to 2 mg/kg haloperidol with PCA. Each signaling response was treated as a unique feature of each animal and the first two principal components (PCs) were plotted (Figure 3). PC1 distinguished iMSN-D2[AAV-βarr] from iMSN-D2[AAV-WT] and iMSN-D2[AAV-Gprot] mice. PC2 distinguished iMSN-D2[AAV-Gprot] from iMSN-D2[AAV-WT] mice, although less robustly. Thus, between the two functionally selective variants, iMSN-D2[AAV-Gprot] mice most resemble iMSN-D2[AAV-WT] in their signaling response to haloperidol. The egr-1 response, though, shows that the β-arrestin-biased variant (iMSN-D2[AAV-βarr]) is capable of transducing a specific aspect of haloperidol-induced changes.

Basic iMSN-D2R-Driven Behaviors Involve Both D2R/G-Protein and D2R/β-Arrestin Signaling

In the classic 'go-no-go' model of the basal ganglia, dopamine neurotransmission through iMSN-D2Rs disinhibits basal ganglia circuits and facilitates motor output (Alexander et al, 1986). Although canonical models of D2R signaling indicate that motor output is driven by G-protein-mediated reduction in intracellular cAMP (Kebabian and Calne, 1979), a role for β-arrestin-mediated signaling has also emerged (Beaulieu et al, 2005; Urs et al, 2012). Here, we sought to objectively assess the role for both D2R/G-protein
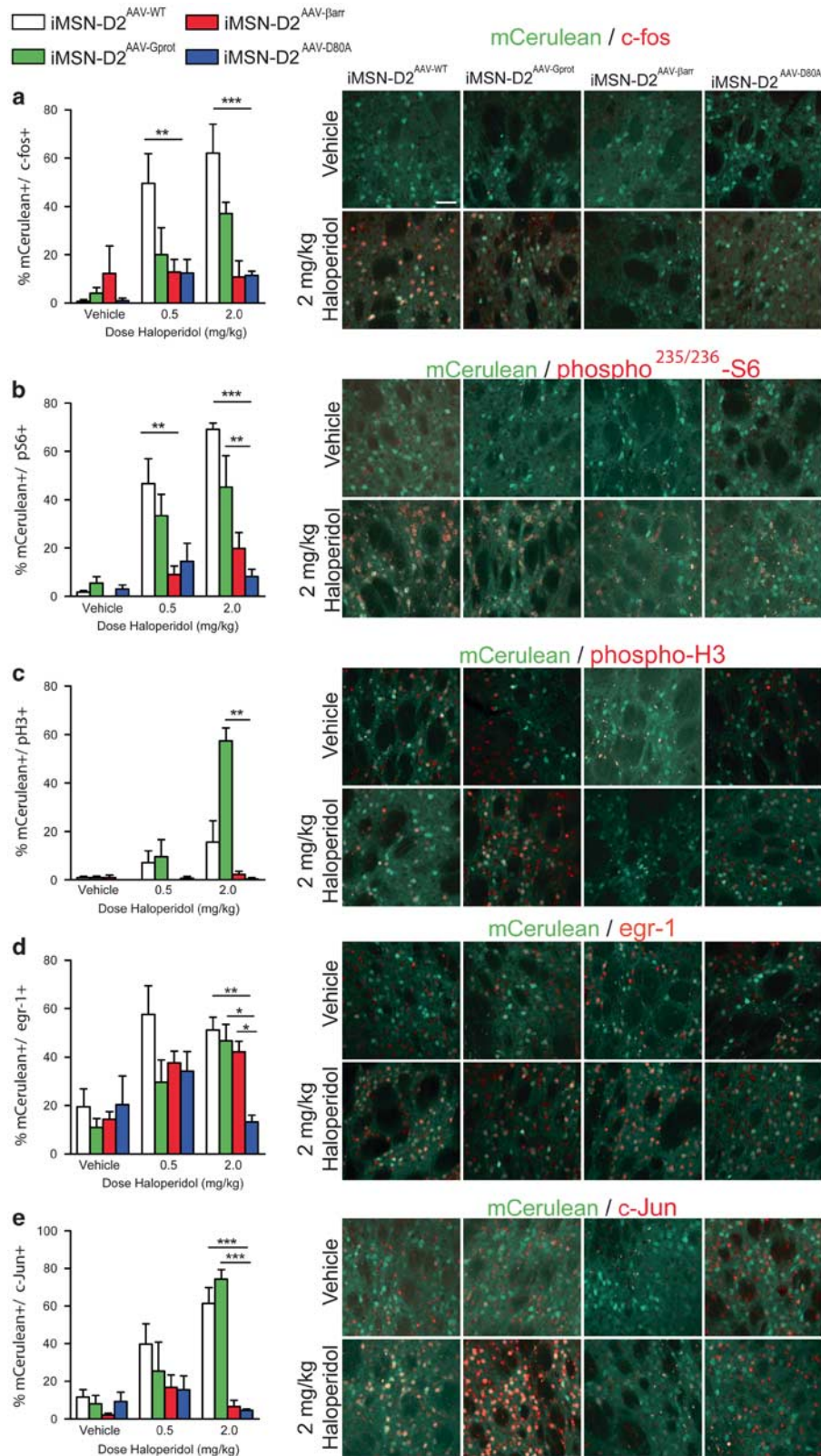
and D2R/β-arrestin signaling in stimulating motor output. We first examined deficits in iMSN-D2[KO] before viral reconstitution to establish that motoric deficits were driven by a lack of iMSN-D2Rs. Indeed, iMSN-D2[KO] mice showed a deficit in open-field behavior (interaction, $F_{2, 28} = 10.5$, $p < 0.001$; Figure 4a), in agreement with others using the same Cre-lox strategy (Kharkwal et al, 2016b; Lemos et al, 2016). Next, we tested the iMSN-D2[AAV] groups for
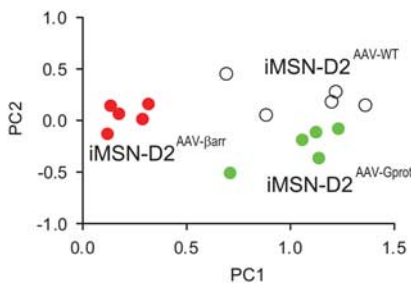
Figure 3 PCA in the cell activation markers over iMSN-D2[AAV-D80A] following 2 mg/kg haloperidol in iMSN-D2[AAV-WT] ($n=5$), iMSN-D2[AAV-βarr] ($n=5$), and iMSN-D2[AAV-Gprot] mice ($n=5$). PC1 distinguishes the iMSN-D2[AAV-βarr] from iMSN-D2[AAV-WT] and iMSN-D2[AAV-Gprot]. PC2 distinguishes iMSN-D2[AAV-WT] from iMSN-D2[AAV-Gprot]. Points represent the signaling responses of individual animals. White = iMSN-D2[AAV-WT], red = iMSN-D2[AAV-βarr], and green = iMSN-D2[AAV-Gprot] mice.

open-field locomotion. Whereas iMSN-D2[AAV-WT] restored open-field locomotion (time, $F_{2, 78}=6.22$, $p<0.05$; Figure 4b), showing a significant difference from iMSN-D2[AAV-D80A] mice, both iMSN-D2[AAV-βarr] and iMSN-D2[AAV-Gprot] mice showed partial restoration of locomotion, with responses between iMSN-D2[AAV-D80A] and iMSN-D2[AAV-WT] mice. These differences could not be explained by differences in D2R expression, as we observed no significant association between locomotion and HA intensity (Supplementary Figure S1). iMSN-D2[KO] also showed a deficit in rearing behavior ($p<0.01$, Figure 4c). iMSN-D2[AAV-WT] showed a trend ($F_{2, 28}=2.47$, $p=0.06$) toward restoring rearing, though similar to open-field locomotion, neither iMSN-D2[AAV-βarr] nor iMSN-D2[AAV-Gprot] fully restored rearing (Figure 4d). Like the cellular c-fos response, neither D2R/G-protein nor D2R/β-arrestin signaling, alone, was sufficient to fully restore locomotion and rearing behavior.

Next, we examined nestlet shredding behavior, a natural rodent behavior that requires coordinated motor skills and is triggered by anxiogenic stimuli (Li *et al*, 2006; Angoa-Perez *et al*, 2013). We hypothesized that iMSN-D2Rs were required for nestlet shredding as they are involved in emotional valence and coordinated motor activity (Baik *et al*, 1995; Richard and Berridge, 2011). Indeed, iMSN-D2[KO] were

deficient in nestlet shredding behavior ($p<0.01$; Figure 4e). Interestingly, iMSN-D2[AAV-Gprot] mice ($F_{3, 49}=3.4$, $p<0.05$), but not the other two active D2R variants, showed significant restoration of this behavior over iMSN-D2[AAV-D80A] mice. Thus, this particular behavior seems to be driven by D2R/G-protein signaling. It is interesting to note that despite the fact that [Gprot]D2R had reduced receptor expression and incomplete locomotor activity, the nestlet shredding phenotype was completely restored. This, along with the sufficiency in haloperidol responses, indicates that [Gprot]D2R is fully functional at lower expression levels.

β-Arrestin Signaling Drives the D2R Phencyclidine Response

Along with basic, exploratory locomotion, dopamine signaling also mediates the psychomotor effect of drugs like amphetamine, cocaine, and phencyclidine (PCP) (Wise and Bozarth, 1987). Although each drug increases presynaptic dopamine release and locomotion, the precise mechanisms differ from drug to drug (Carboni *et al*, 1989; French *et al*, 1993; Covey *et al*, 2013; Daberkow *et al*, 2013). How these differing mechanisms affect D2R activation and whether biased signaling plays any role in distinguishing one drug response from another is not known. To investigate these questions, we tested the locomotor response to amphetamine, cocaine, and PCP in iMSN-D2[KO] mice and iMSN-D2[AAV] groups. We observed deficient responses to 3 mg/kg amphetamine (interaction, $F_{29, 406}=26.5$, $p<0.001$; Figure 5a), 10 mg/kg cocaine (interaction, $F_{29, 406}=11.7$, $p<0.001$; Figure 5c), and 6 mg/kg PCP in iMSN-D2[KO] mice (interaction, $F_{87, 696}=6.72$, $p<0.01$; Figure 5e), verifying previously published results (Dobbs *et al*, 2016; Urs *et al*, 2016). iMSN-D2[AAV-WT] mice showed restoration of amphetamine-induced locomotion (interaction, $F_{87, 1131}=2.80$, $p<0.01$ where indicated; Figure 5b). iMSN-D2[AAV-βarr] and iMSN-D2[AAV-Gprot] mice demonstrated only partial restoration of amphetamine-induced locomotion (Figure 5b). With cocaine, however, iMSN-D2[AAV-WT] (interaction, $F_{87, 696}=6.75$, $p<0.001$), iMSN-D2[AAV-βarr] ($p<0.001$), and iMSN-D2[AAV-Gprot] mice ($p<0.01$) all showed significant restoration of locomotion (Figure 5d). Cocaine-induced locomotion in iMSN-D2[AAV-WT] required D2R expression in both dorsal and ventral striatum,
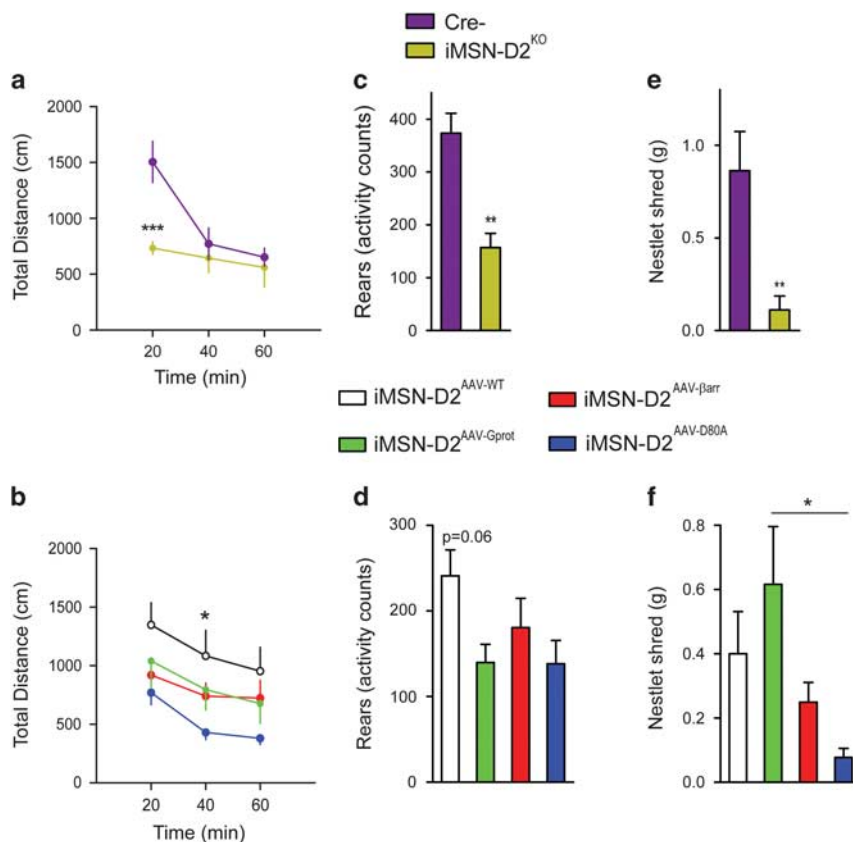
Figure 4 Examination of iMSN-D2R-biased signaling pathways in basic D2R-driven behaviors. (a) iMSN-D2^{KO} and Cre- littermate controls were tested in a novel open field for 1 h ($n = 8$/genotype). Locomotion was significantly reduced in iMSN-D2^{KO} (two-way repeated-measures ANOVA of genotype × time interaction with Bonferroni *post hoc* test, ***$p < 0.001$). (b) Next, iMSN-D2^{AAV-WT} ($n = 10$), iMSN-D2$^{AAV-Gprot}$ ($n = 12$), iMSN-D2$^{AAV-\beta arr}$ ($n = 12$), and iMSN-D2$^{AAV-D80A}$ ($n = 9$) were tested in the novel open field. iMSN-D2^{AAV-WT} showed restoration of open-field locomotion compared with iMSN-D2$^{AAV-D80A}$ (two-way repeated-measures ANOVA on effect of time with Bonferroni *post hoc* test, *$p < 0.05$). iMSN-D2$^{AAV-Gprot}$ and iMSN-D2$^{AAV-\beta arr}$ mice showed intermediate restoration effects, with no significant difference found between these viral genotypes and iMSN-D2^{AAV-WT} or iMSN-D2$^{AAV-D80A}$ mice. (c) Rearing was assessed concurrently to locomotion. Rearing was significantly reduced in iMSN-D2^{KO} compared with Cre- littermates (Student's *t*-test, **$p < 0.01$). (d) Rearing showed nonsignificant trend toward restoration in iMSN-D2^{AAV-WT} compared with iMSN-D2$^{AAV-D80A}$ mice (ANOVA with Bonferroni *post hoc* test $p = 0.06$), but not in iMSN-D2$^{AAV-Gprot}$ and iMSN-D2$^{AAV-\beta arr}$ mice. (e) Nestlet shredding behavior was assessed in iMSN-D2^{KO} and Cre- littermate controls. iMSN-D2^{KO} showed a reduction in this behavior (Student's *t*-test, **$p < 0.01$). (f) Nestlet shredding was significantly restored in iMSN-D2$^{AAV-Gprot}$ mice (ANOVA with Bonferroni *post hoc* test, *$p < 0.05$). Values represent mean ± SEM.

as expression of D2R individually in these subregions was insufficient in restoring locomotion (Supplementary Figure S3). Intriguingly, PCP-induced locomotion was potentiated in iMSN-D2$^{AAV-\beta arr}$ (interaction, $F_{87, 696} = 6.72$, $p < 0.01$), whereas iMSN-D2$^{AAV-Gprot}$ showed minimal restoration (Figure 5f). These findings illustrate selective roles for D2R/G-protein and D2R/β-arrestin signaling in the locomotor response to these three drugs, with a surprisingly robust role for D2R/β-arrestin signaling in PCP-induced locomotion. Interestingly, iMSN-D2^{KO} mice showed normal conditioned place preference for cocaine, illustrating the specificity of the iMSN-D2^{KO} effect to acute psychomotor effects, at least for cocaine (Supplementary Figure S4).

DISCUSSION

D2Rs are critical for many normal neurobehavioral functions and are a target of therapeutics for Parkinson's disease, schizophrenia, and other basal ganglia-related disorders.

Since the discovery of β-arrestin-mediated D2R signaling, a growing body of literature has demonstrated biased D2R signaling and its importance in various contexts (Beaulieu *et al*, 2005; Masri *et al*, 2008; Allen *et al*, 2011; Urs *et al*, 2015; Urs *et al*, 2016). Few of these studies, however, have examined biased D2R signaling in a manner that does not disrupt pleiotropic signaling proteins. Using biased receptor viral reconstitution, we examined the functional consequences of biased D2R signaling in a way that preserves non-dopaminergic signaling and limits our manipulations to iMSNs. We show that cellular responses to D2R antagonism are mostly driven by D2R/G-protein signaling, though D2R/β-arrestin signaling contributes as well. Behaviorally, we show that neither D2R/G-protein nor D2R/β-arrestin signaling, alone, can drive locomotion. Finally, we show that D2R/β-arrestin signaling potentiates phencyclidine-induced psychomotor effects. These data highlight the importance of iMSN-D2Rs for neurobehavioral functions and demonstrate GPCR functional selectivity with unprecedented precision.
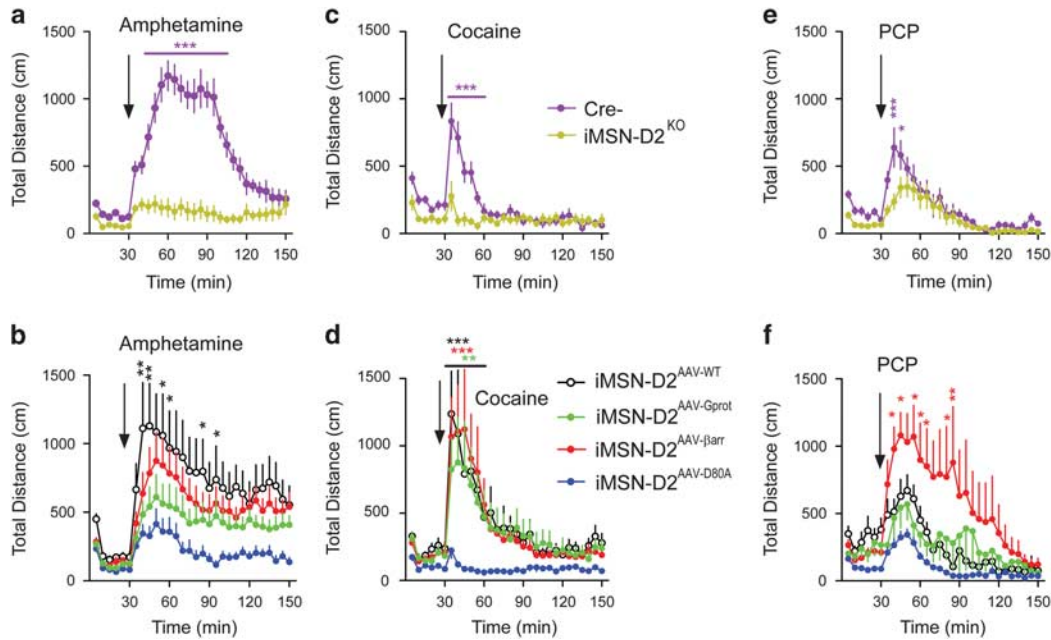
Figure 5 Examination of iMSN-D2R-biased signaling pathways in psychomotor drug effects. (a) iMSN-D2^{KO} ($n=8$) and Cre- ($n=8$) littermate controls were tested for their locomotor response to 3 mg/kg amphetamine. Amphetamine-induced locomotion was significantly reduced in iMSN-D2^{KO} mice following 3 mg/kg compared with Cre- controls (two-way repeated-measures ANOVA on genotype × time interaction with Bonferroni *post hoc* tests within time points, ***p < 0.001). (b) Next, iMSN-D2^{AAV-WT} ($n=10$), iMSN-D2$^{AAV-Gprot}$ ($n=12$), iMSN-D2$^{AAV-\beta arr}$ ($n=12$), and iMSN-D2$^{AAV-D80A}$ ($n=9$) were tested for amphetamine-induced locomotion. iMSN-D2^{AAV-WT} mice showed significant restoration of amphetamine-induced locomotion over iMSN-D2$^{AAV-D80A}$ (two-way repeated-measures ANOVA on viral genotype × time interaction with Bonferroni *post hoc* tests, *p < 0.05 and **p < 0.01). iMSN-D2$^{AAV-Gprot}$ and iMSN-D2$^{AAV-\beta arr}$ mice showed intermediate restoration effects, with no significant difference found between these viral genotypes and iMSN-D2^{AAV-WT} or iMSN-D2$^{AAV-D80A}$ mice. (c) Locomotion was significantly reduced in iMSN-D2^{KO} following 10 mg/kg cocaine (two-way RMANOVA on genotype × time interaction with Bonferroni *post hoc* tests, ***p < 0.001). (d) iMSN-D2^{AAV-WT} ($n=6$), iMSN-D2$^{AAV-Gprot}$ ($n=8$), iMSN-D2$^{AAV-\beta arr}$ ($n=8$), and iMSN-D2$^{AAV-D80A}$ ($n=6$) were similarly tested following 10 mg/kg cocaine. The iMSN-D2^{AAV-WT}, iMSN-D2$^{AAV-Gprot}$, and iMSN-D2$^{AAV-\beta arr}$ mice all showed significant restoration of cocaine induced locomotion (two-way repeated-measures ANOVA on genotype × time interaction with Bonferroni *post hoc* tests, **p < 0.01 and ***p < 0.001). (e) Finally, PCP-induced locomotion was tested in iMSN-D2^{KO} and Cre- mice that was significantly reduced in iMSN-D2^{KO} mice (two-way repeated-measures ANOVA on genotype × time interaction with Bonferroni *post hoc* tests, *p < 0.05 and **p < 0.001). (f) iMSN-D2$^{AAV-\beta arr}$ mice ($n=8$) showed significant restoration of PCP-induced locomotion over iMSN-D2$^{AAV-D80A}$ mice ($n=6$) (two-way repeated-measures ANOVA on genotype × time interaction with Bonferroni *post hoc* tests, *p < 0.05 and **p < 0.01 Bonferroni *post hoc* tests). iMSN-D2^{AAV-WT} ($n=6$) and iMSN-D2$^{AAV-Gprot}$ mice ($n=8$), however, only showed intermediate restoration, not significantly differing from iMSN-D2$^{AAV-D80A}$ mice. Values represent mean ± SEM.

G-Protein-Biased Haloperidol Responses

Our finding that most of the cell signaling response to haloperidol is driven by blockade of acute D2R/G-protein signaling is in concert with existing data. Several studies have illustrated the importance of adenylyl cyclase–cAMP–PKA–DARPP32 signaling for haloperidol-induced phosphorylation of S6 and H3, and the expression of c-fos and egr-1 (Bertran-Gonzalez et al, 2008; Bertran-Gonzalez et al, 2009; Valjent et al, 2011; Bonito-Oliva et al, 2013). On the other hand, ERK 1/2, which is activated by both D2R/G-protein and D2R/β-arrestin signaling (Peterson et al, 2015), is critical for haloperidol-induced signaling as well (Bertran-Gonzalez et al, 2008; Valjent et al, 2011). Our approach confirms that the metabolic changes induced by haloperidol are mostly due to D2R/G-protein signaling disruption. These data are in support of a model where antipsychotics mediate gene transcriptional changes and long-term effects through antagonism of D2R/G-protein signaling (Bateup et al, 2010; Allen et al, 2011), whereas antagonism of D2R/β-arrestin signaling mediates nontranscriptional changes to cell physiology that mediate the reduction in the positive symptoms of schizophrenia (Masri et al, 2008; Allen et al, 2011; Urs et al, 2012). An important update to this model is our finding

that antagonism of D2R/β-arrestin signaling is capable of driving haloperidol-induced egr-1 expression. Thus, some overlap of D2R/G-protein and D2R/β-arrestin signaling likely occurs. Furthermore, the inability of iMSN-D2R$^{AAV-Gprot}$ mice to reconstitute c-fos expression points to the necessity for cooperation between D2R/G-protein and D2R/β-arrestin signaling for certain neuronal changes. As it is becoming understood that iMSNs are a genetically heterogeneous cell population (Gokce et al, 2016), the biased effects of haloperidol on unique subpopulations of iMSNs will be interesting to dissect in the future.

A Range of Signaling Modes in D2R-Driven Behaviors

Our finding that reconstitution of D2R/β-arrestin or D2R/G-protein signaling only partially reconstitutes open-field locomotion, individually, are interesting in the context of Parkinson's disease. Recent studies using iMSN-D2R^{KO} mice show that loss of D2Rs in iMSNs mimics parkinsonian hypokinesia by enhancing GABAergic transmission from iMSNs to GPe, and by enhancing iMSN lateral inhibition of dMSNs (Dobbs et al, 2016; Lemos et al, 2016). Our data point to a cooperative role for D2R/β-arrestin and D2R/G-protein

signaling in mediating these physiological effects and driving open-field locomotion. Future work could focus on determining how each signaling pathway contributes to the maintenance of normal iMSN physiology, though targeting one biased D2R signaling pathway is unlikely to be a 'silver bullet' for reversing parkinsonian symptoms. Our nestlet shredding data, however, illustrate that a single biased D2R signaling pathway is capable of driving a D2R-dependent behavior on its own.

Finally, we illustrated the complex role that biased D2R signaling plays in mediating psychotropic drug responses. Amphetamine, cocaine, and PCP require iMSN-D2Rs to mediate their acute effect on locomotion, making the viral reconstitution approach ideal for elucidating the biased D2R signaling mechanisms of these drugs. Despite a similar requirement of iMSN-D2Rs, amphetamine, cocaine, and PCP engage biased D2R signaling in different ways. Amphetamine, like unstimulated open-field locomotion, requires a combination of D2R/β-arrestin and D2R/G-protein signaling as neither iMSN-D2R$^{\text{AAV-Gprot}}$ nor iMSN-D2R$^{\text{AAV-}\beta\text{arr}}$ mice fully restore amphetamine-induced locomotion. On the other hand, iMSN-D2R$^{\text{AAV-Gprot}}$ and iMSN-D2R$^{\text{AAV-}\beta\text{arr}}$ both individually restored cocaine-induced locomotion. Both amphetamine and cocaine directly increase dopamine transmission. Amphetamine, though, is a so-called dopamine 'releaser', depleting vesicular stores and promoting nonexocytotic dopamine efflux via reverse transport, whereas cocaine merely inhibits the dopamine transporter (Sulzer, 2011). These differing pharmacologies translate to a difference in their effects on tonic dopamine signaling. Although both drugs enhance phasic dopamine signals, amphetamine also enhances tonic dopamine signaling by depleting the reserve pool of dopamine in the presynaptic terminal (Covey *et al*, 2013; Daberkow *et al*, 2013). Our results raise the intriguing possibility that biased D2R signaling, at least in part, translates the difference between tonic and phasic dopamine signals. For instance, although the phasic dopamine signal elicited by cocaine stimulation may initiate a D2R signal that either D2R/β-arrestin or D2R/G-protein are capable of transducing, say the activation of ERK1/2 (Peterson *et al*, 2015), the amphetamine-induced increase in tonic dopamine signal may engage cooperative D2R/G-protein and D2R/β-arrestin signaling that stimulates ERK1/2 and combinations of other signaling networks. Further work will be required to test these hypotheses, but these data lend support to different effects of cocaine and amphetamine on iMSN signaling and plasticity (Jedynak *et al*, 2016). Contrasting both cocaine and amphetamine-induced locomotion, PCP-induced locomotion is mostly driven by D2R/β-arrestin signaling. This difference may reflect the role of D2R/β-arrestin signaling in integrating glutamatergic and phasic dopamine signals elicited by PCP (French *et al*, 1993), and a case where the homeostatic balance between G-protein and β-arrestin signaling is shifted toward β-arrestin bias. Furthermore, as PCP-induced locomotion is a long-standing model of schizophrenic symptoms, these data support an approach that targets D2R/β-arrestin signaling for the treatment of schizophrenia (Allen *et al*, 2011; Urs *et al*, 2016). Finally, it is important to note that only single doses of these drugs were tested; full dose responses may reveal more nuance to the roles of these signaling pathways.

CONCLUSIONS

In summary, this study utilized a viral reconstitution approach for studying biased D2R signaling with cell type-specific resolution. The work here highlights the complexity of D2R signaling within iMSNs in the context of behavioral, pharmacological, and physiological functions. These findings have the potential to shape strategies focused on biased D2R pharmacotherapies for a range of brain disorders.

FUNDING AND DISCLOSURE

REFERENCES

Alexander GE, DeLong MR, Strick PL (1986). Parallel organization of functionally segregated circuits linking basal ganglia and cortex. *Annu Rev Neurosci* **9**: 357–381.

Allen JA, Yost JM, Setola V, Chen X, Sassano MF, Chen M *et al* (2011). Discovery of beta-arrestin-biased dopamine D2 ligands for probing signal transduction pathways essential for antipsychotic efficacy. *Proc Natl Acad Sci USA* **108**: 18488–18493.

Angoa-Perez M, Kane MJ, Briggs DI, Francescutti DM, Kuhn DM (2013). Marble burying and nestlet shredding as tests of repetitive, compulsive-like behaviors in mice. *J Vis Exp* **82**: 50978.

Bahrami S, Drablos F (2016). Gene regulation in the immediate-early response process. *Adv Biol Regul* **62**: 37–49.

Baik JH, Picetti R, Saiardi A, Thiriet G, Dierich A, Depaulis A *et al* (1995). Parkinsonian-like locomotor impairment in mice lacking dopamine D2 receptors. *Nature* **377**: 424–428.

Bateup HS, Santini E, Shen W, Birnbaum S, Valjent E, Surmeier DJ *et al* (2010). Distinct subclasses of medium spiny neurons differentially regulate striatal motor behaviors. *Proc Natl Acad Sci USA* **107**: 14845–14850.

Beaulieu JM, Sotnikova TD, Marion S, Lefkowitz RJ, Gainetdinov RR, Caron MG (2005). An Akt/beta-arrestin 2/PP2A signaling complex mediates dopaminergic neurotransmission and behavior. *Cell* **122**: 261–273.

Bello EP, Mateo Y, Gelman DM, Noain D, Shin JH, Low MJ *et al* (2011). Cocaine supersensitivity and enhanced motivation for reward in mice lacking dopamine D2 autoreceptors. *Nat Neurosci* **14**: 1033–1038.

Bertran-Gonzalez J, Bosch C, Maroteaux M, Matamales M, Herve D, Valjent E *et al* (2008). Opposing patterns of signaling activation in dopamine D1 and D2 receptor-expressing striatal neurons in response to cocaine and haloperidol. *J Neurosci* **28**: 5671–5685.

Bertran-Gonzalez J, Hakansson K, Borgkvist A, Irinopoulou T, Brami-Cherrier K, Usiello A *et al* (2009). Histone H3 phosphorylation is under the opposite tonic control of dopamine D2 and adenosine A2A receptors in striatopallidal neurons. *Neuropsychopharmacology* **34**: 1710–1720.

Bohn LM, Gainetdinov RR, Lin FT, Lefkowitz RJ, Caron MG (2000). Mu-opioid receptor desensitization by beta-arrestin-2 determines morphine tolerance but not dependence. *Nature* **408**: 720–723.

Bonito-Oliva A, Pallottino S, Bertran-Gonzalez J, Girault JA, Valjent E, Fisone G (2013). Haloperidol promotes mTORC1-dependent phosphorylation of ribosomal protein S6 via dopamine- and cAMP-regulated phosphoprotein of 32 kDa and inhibition of protein phosphatase-1. *Neuropharmacology* 72: 197–203.

Carboni E, Imperato A, Perezzani L, Di Chiara G (1989). Amphetamine, cocaine, phencyclidine and nomifensine increase extracellular dopamine concentrations preferentially in the nucleus accumbens of freely moving rats. *Neuroscience* 28: 653–661.

Carlsson A (1978). Antipsychotic drugs, neurotransmitters, and schizophrenia. *Am J Psychiatry* 135: 165–173.

Centonze D, Grande C, Usiello A, Gubellini P, Erbs E, Martin AB et al (2003). Receptor subtypes involved in the presynaptic and postsynaptic actions of dopamine on striatal interneurons. *J Neurosci* 23: 6245–6254.

Covey DP, Juliano SA, Garris PA (2013). Amphetamine elicits opposing actions on readily releasable and reserve pools for dopamine. *PLoS ONE* 8: e60763.

Daberkow DP, Brown HD, Bunner KD, Kraniotis SA, Doellman MA, Ragozzino ME et al (2013). Amphetamine paradoxically augments exocytotic dopamine release and phasic dopamine signals. *J Neurosci* 33: 452–463.

Dobbs LK, Kaplan AR, Lemos JC, Matsui A, Rubinstein M, Alvarez VA (2016). Dopamine regulation of lateral inhibition between striatal neurons gates the stimulant actions of cocaine. *Neuron* 90: 1100–1113.

French ED, Mura A, Wang T (1993). MK-801, phencyclidine (PCP), and PCP-like drugs increase burst firing in rat A10 dopamine neurons: comparison to competitive NMDA antagonists. *Synapse* 13: 108–116.

Gerfen CR, Engber TM, Mahan LC, Susel Z, Chase TN, Monsma FJ et al (1990). D1 and D2 dopamine receptor regulated gene expression of striatonigral and striatopalidal neurons. *Science* 250: 1429–1432.

Gokce O, Stanley G, Treutlein B, Neff NF, Camp GJ, Malenka RC et al (2016). Cellular taxonomy of the mouse striatum as revealed by single-cell RNA-Seq. *Cell Rep* 16: 1126–1137.

Jedynak J, Hearing M, Ingebretson A, Ebner SR, Kelly M, Fischer RA et al (2016). Cocaine and amphetamine induce overlapping but distinct patterns of AMPAR plasticity in nucleus accumbens medium spiny neurons. *Neuropsychopharmacology* 41: 464–476.

Kane J, Honigfeld G, Singer J, Meltzer H (1988). Clozapine for the treatment-resistant schizophrenic. A double-blind comparison with chlorpromazine. *Arch Gen Psychiatry* 45: 789–796.

Kebabian JW, Calne DB (1979). Multiple receptors for dopamine. *Nature* 277: 93–96.

Kharkwal G, Brami-Cherrier K, Lizardi-Ortiz JE, Nelson AB, Ramos M, Del Barrio D et al (2016a). Parkinsonism driven by antipsychotics originates from dopaminergic control of striatal cholinergic interneurons. *Neuron* 91: 67–78.

Kharkwal G, Radl D, Lewis R, Borrelli E (2016b). Dopamine D2 receptors in striatal output neurons enable the psychomotor effects of cocaine. *Proc Natl Acad Sci USA* 113: 11609–11614.

Lemos JC, Friend DM, Kaplan AR, Shin JH, Rubinstein M, Kravitz AV et al (2016). Enhanced GABA transmission drives bradykinesia following loss of dopamine D2 receptor signaling. *Neuron* 90: 824–838.

Li X, Morrow D, Witkin JM (2006). Decreases in nestlet shredding of mice by serotonin uptake inhibitors: comparison with marble burying. *Life Sci* 78: 1933–1939.

Lieberman JA, Stroup TS, McEvoy JP, Swartz MS, Rosenheck RA, Perkins DO et al (2005). Effectiveness of antipsychotic drugs in patients with chronic schizophrenia. *New Engl J Med* 353: 1209–1223.

Masri B, Salahpour A, Didriksen M, Ghisi V, Beaulieu JM, Gainetdinov RR et al (2008). Antagonism of dopamine D2 receptor/beta-arrestin 2 interaction is a common property of clinically effective antipsychotics. *Proc Natl Acad Sci USA* 105: 13656–13661.

Nishi A, Snyder GL, Greengard P (1997). Bidirectional regulation of DARPP-32 phosphorylation by dopamine. *J Neurosci* 17: 8147–8155.

Peterson SM, Pack TF, Wilkins AD, Urs NM, Urban DJ, Bass CE et al (2015). Elucidation of G-protein and beta-arrestin functional selectivity at the dopamine D2 receptor. *Proc Natl Acad Sci USA* 112: 7097–7102.

Richard JM, Berridge KC (2011). Nucleus accumbens dopamine/ glutamate interaction switches modes to generate desire versus dread: D(1) alone for appetitive eating but D(1) and D(2) together for fear. *J Neurosci* 31: 12866–12879.

Rogue P, Vincendon G (1992). Dopamine D2 receptor antagonists induce immediate early genes in the rat striatum. *Brain Res Bull* 29: 469–472.

Seeman P, Lee T, Chau-Wong M, Wong K (1976). Antipsychotic drug doses and neuroleptic/dopamine receptors. *Nature* 261: 717–719.

Sheng M, Greenberg ME (1990). The regulation and function of c-fos and other immediate early genes in the nervous system. *Neuron* 4: 477–485.

Sulzer D (2011). How addictive drugs disrupt presynaptic dopamine neurotransmission. *Neuron* 69: 628–649.

Urs NM, Bido S, Peterson SM, Daigle TL, Bass CE, Gainetdinov RR et al (2015). Targeting beta-arrestin2 in the treatment of L-DOPA-induced dyskinesia in Parkinson's disease. *Proc Natl Acad Sci USA* 112: E2517–E2526.

Urs NM, Gee SM, Pack TF, McCorvy JD, Evron T, Snyder JC et al (2016). Distinct cortical and striatal actions of a beta-arrestin-biased dopamine D2 receptor ligand reveal unique antipsychotic-like properties. *Proc Natl Acad Sci USA* 113: E8178–E8186.

Urs NM, Snyder JC, Jacobsen JP, Peterson SM, Caron MG (2012). Deletion of GSK3beta in D2R-expressing neurons reveals distinct roles for beta-arrestin signaling in antipsychotic and lithium action. *Proc Natl Acad Sci USA* 109: 20732–20737.

Valjent E, Bertran-Gonzalez J, Bowling H, Lopez S, Santini E, Matamales M et al (2011). Haloperidol regulates the state of phosphorylation of ribosomal protein S6 via activation of PKA and phosphorylation of DARPP-32. *Neuropsychopharmacology* 36: 2561–2570.

Weinberger DR (1987). Implications of normal brain development for the pathogenesis of schizophrenia. *Arch Gen Psychiatry* 44: 660–669.

Weiner DM, Levey AI, Sunahara RK, Niznik HB, O'Dowd BF, Seeman P et al (1991). D1 and D2 dopamine receptor mRNA in rat brain. *Proc Natl Acad Sci USA* 88: 1859–1863.

Whalen EJ, Rajagopal S, Lefkowitz RJ (2011). Therapeutic potential of beta-arrestin- and G protein-biased agonists. *Trends Mol Med* 17: 126–139.

Wise RA, Bozarth MA (1987). A psychomotor stimulant theory of addiction. *Psychol Rev* 94: 469–492.

Xiao X, Li J, Samulski RJ (1998). Production of high-titer recombinant adeno-associated virus vectors in the absence of helper adenovirus. *J Virol* 72: 2224–2232.

Supplementary Information accompanies the paper on the Neuropsychopharmacology website (http://www.nature.com/npp)